International Journal of Concrete
Structures and Materials

RESEARCH   **Open Access**

Energy Absorption Characteristics of PVC Coarse Aggregate Concrete under Impact Load

Shi Hu[*], Huaming Tang and Shenyao Han

Abstract

In this paper, polyvinyl chloride (PVC) coarse aggregate with different mixing contents is used to solve the problems of plastic pollution, low energy absorption capacity and poor damage integrity, which provides an important reference for PVC plastic concrete used in the initial support structures of highway tunnels and coal mine roadway. At the same time, the energy absorption characteristics and their relationship under different impact loads are studied, which provides an important reference for predicting the energy absorption characteristics of concrete under other PVC aggregate content or higher impact speed. This study replaced natural coarse aggregate in concrete with different contents and equal volume of well-graded flaky PVC particles obtained by crushing PVC soft board. Also, slump, compression, and splitting strength tests, a free falling low-speed impact test of steel balls and a high-speed impact compression test of split Hopkinson pressure bar (SHPB) were carried out. Results demonstrate that the static and dynamic compressive strength decreases substantially, and the elastic modulus and slump decrease slowly with the increase of the mixing amount of PVC aggregate (0–30%). However, the energy absorption rate under low-speed impact and the specific energy absorption per MPa under high-speed impact increase obviously, indicating that the energy absorption capacity is significantly enhanced. Regardless of the mixing amount of PVC aggregate, greater strain rate can significantly enhance the dynamic compressive strength and the specific energy absorption per MPa. After the uniaxial compression test or the SHPB impact test, the relative integrity of the specimen is positively correlated with the mixing amount of PVC aggregate. In addition, the specimens are seriously damaged with the increase of the impact strain rate. When the PVC aggregate content is 20%, the compressive strength and splitting strength of concrete are 33.8 MPa and 3.26 MPa, respectively, the slump is 165 mm, the energy absorption rate under low-speed impact is 89.5%, the dynamic compressive strength under 0.65 Mpa impact air pressure is 58.77 mpa, and the specific energy absorption value per MPa is 13.33, which meets the requirements of shotcrete used in tunnel, roadway support and other impact loads. There is a linear relationship between the energy absorption characteristics under low-speed impact and high-speed impact. The greater the impact pressure, the larger the slope of the fitting straight line. The slope and intercept of the fitting line also show a good linear relationship with the increase of impact pressure. The conclusions can be used to predict the energy absorption characteristics under different PVC aggregate content or higher-speed impact pressure, which can provide important reference for safer, more economical, and environmental protection engineering structure design.

Keywords: flake polyvinyl chloride particles, good gradation, compressive strength, splitting tensile strength, energy absorption, impact load

1 Introduction

Waste plastics have brought about serious pollution around the world. Replacing aggregate in concrete with plastics such as PET and PVC is a simple and environmentally friendly waste plastics recycling method (Opon

*Correspondence: aust_shihu@163.com
School of Civil Engineering and Architecture, Anhui University of Science and Technology, No. 168 Taifeng Road, Huainan 232001, China

Hu *et al. Int J Concr Struct Mater*   (2021) 15:26

Page 2 of 16

& Henry, 2019). Although mixing more plastics can obviously decrease the strength of plastic concrete and increase the water absorption rate (Hu & Xu, 2020a, 2020b), it has the advantages of light weight, elastic shock absorption, high energy absorption, frost resistance, impact resistance and wear resistance, making it applicable to non-load-bearing structural engineering projects (Siddique et al., 2008). However, plastic concrete is seldom used in engineering projects with frequent impact loads, such as military protection (Bui et al. 2018), airport pavement (Senhadji et al. 2019) and deep roadway support (Siddique et al., 2008). Therefore, it is of great practical significance to thoroughly study the energy absorption characteristics of plastic concrete under impact loads (Mohammed et al., 2019). Scholars have carried out a great number of relevant studies.

Mohammed et al. (2019) replaced sand or stones in concrete with PVC aggregates with different particle sizes obtained by crushing PVC plates, which not only decreased the slump and strength of concrete, but also improved the brittleness. Although the raw materials were obtained by crushing the PVC plates twice, the grain size was similar and the grading effect was poor. Al-Tayeb et al. (2017) used waste plastics of vehicles as substitute aggregate, finding that increasing the content of aggregate can significantly improve the impact resistance under low-speed impact load, under 15% content, the impact damage energy is 88.23% higher than that of the reference group. Saxena et al. (2018) chopped PET bottles to replace natural aggregates in concrete. Although the concrete had poor compressive strength, its impact resistance was improved with the increase of the mixing amount of PET plastics, and the energy absorption capacity was enhanced, after adding 20% pet coarse aggregate, the energy absorption value increased by 378%. Drop weight impact test is also widely used in fiber reinforced concrete. Chen et al. (2011) used steel fiber and steel reinforcement to strengthen concrete, adding 35 Kg/M^3 steel fiber and 6 steel bars with a diameter of 12 mm, and finally the number of impact damage reached 1400 times, nearly 77 times higher than that of ordinary concrete. Cao et al. (2018) used the hybrid fiber reinforcement method of PVA and steel fiber, and the final number of impact damage reached 450 times. Therefore, for concrete specimens with strong anti-impact ability, the error of energy absorption calculated using the drop hammer impact test is large, and the number of impact is too many, and the test equipment is easy to be damaged. Therefore, scholars began to use steel ball free falling impact to test energy absorption characteristics. Hu and Xu (2020a, b) replaced natural fine aggregate in concrete with equal volume of well-graded recycled PVC particles. The strength and unloading elastic modulus decreased

with the increase of the replacement amount, while the ductility and energy absorption capacity were enhanced, the maximum energy absorption rate reached 91.11% (30% content). Meanwhile, to study the energy absorption characteristics of concrete under high-speed impact load and accurately capture the stress–strain curve of the specimens, the energy absorption characteristics of the concrete were evaluated according to the SHPB test results. Xuan et al. (2019) indicated that ABS plastic concrete had stronger ductility in the failure mode, and the stress–strain curve had greater peak strain. Increasing the content of plastics can significantly decrease the dynamic compressive strength of concrete, and the energy dissipation density also showed a downtrend, compared with the baseline group, the energy dissipation density increased by 7.8% under the 20% dosage, and the energy dissipation density also increased obviously with the increase of impact pressure.

Feng et al. (2018) tested dynamic splitting tensile of rubber concrete using 100 mm SHPB system and falling hammer. By characterizing tensile strength and energy absorption, it was found that rubber concrete had better energy absorption performance than common concrete under high strain rate. In the case of medium strain rate (falling hammer), when the mixing amount of rubber was about 30%, rubber concrete had the best energy absorption and impact resistance. The energy absorption value is 78.6 J. Under the same energy absorption value, the absorption time is the longest, which is three times that of ordinary concrete. Pham et al. (2020) found that the crack growth, specimen failure integrity and energy absorption capacity of rubber concrete with 0–30% mixing content were significantly higher than those of ordinary concrete. They believed that the energy absorption capacity of rubber concrete could be accurately reflected using the normalized energy absorption value of compressive strength, which was 54–79% higher than that of ordinary concrete. Li et al. (2016) studied the dynamic mechanical properties of concrete reinforced by hybrid fiber of PVA and steel fiber, and used specific energy absorption value (SEA) as the evaluation index of energy absorption, and the greater the strain rate, the greater the energy absorption value.

The existing studies of replacing aggregate in concrete with plastic particles have all centered on plastic fine particles with single particle size. The relationship between energy absorption characteristics of concrete under steel ball free falling low-speed impact load and SHPB high-speed impact load is seldom studied. The study of this relationship can help us only know the energy absorption characteristics under low-speed impact, but can predict different energy absorption characteristics under high-speed impact, so we can avoid carrying

Hu *et al. Int J Concr Struct Mater* (2021) 15:26

Page 3 of 16

out complex high-speed impact test. In addition, it can be used to predict the energy absorption characteristics under low-speed and high-speed impact under different content, so that it can select the best and most environmentally friendly PVC aggregate content according to the requirements of different engineering energy absorption characteristics.

To this end, this study used equal volume of well-graded flaky PVC particles obtained by crushing waste PVC soft boards to replace crushed stone in concrete. The physical properties, mechanical properties, and energy absorption characteristics under different impact loads were further studied and discussed, determine the optimal PVC aggregate content of PVC plastic concrete meeting the requirements of highway tunnel and coal mine roadway shotcrete. Moreover, the relationship between energy absorption characteristics of concrete under low-speed impact and high-speed impact was investigated. In the future, the energy absorption characteristics under high-speed impact or different PVC aggregate content can be predicted, which can provide important reference for safer, economic and environmental protection engineering structure design.

2 Test Part
2.1 Materials
P.O42.5 Portland cement produced by Anhui Huainan Conch Cement Plant was used, which conforms to GB175-2018 Specification. The fine aggregate was natural medium sand with the maximum particle size of 4.75 mm and the fineness modulus of 2.68 in Huaihe River, conforming to the GB/T14684-2011 specification. The coarse aggregate was granite macadam with continuous grading of 4.75–16 mm, which conformed to GB/T14685-2011 specification. The tap water in the laboratory was used. PVC aggregate was PVC soft board which can be taken as the insulation pad

of workbench, anti-corrosion floor or advertisement board, as shown in Fig. 1a. It was first crushed to flaky particles with the particle size of 4.75–14 mm, density of 1.29 g/cm^3, thickness of about 0.5 mm and tensile strength greater than 14.02 MPa, and then sieved to obtain well-graded PVC particles (the ratio of the particles with the five particle sizes is 1: 1: 1: 1:1), as shown in Fig. 1b. The curve gradation curve is shown in Fig. 1c below, where the specified particle gradation range is from GB/T 14,685−2011.
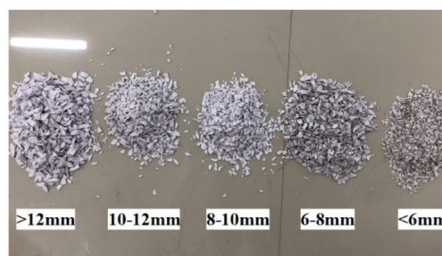
2.2 Concrete Specimen Preparation
On the basis of C30 ordinary concrete, the mixing ratios were designed according to JGJ55-2011, and the water–cement ratio was 0.48. Internal doping method was used to replace gravel with an equal volume of PVC coarse aggregate, and the replacement rates were 0, 5%, 10%, 15%, 20% and 30%, respectively. The mixing ratios are listed in Table 1.

Three 100 mm × 100 mm × 100 mm cubic specimens, three 150 mm × 150 mm × 150 mm cubic specimens and thirteen cylindrical specimens with 70 mm in diameter × 35 mm in height were prepared for the concrete with the above six mixing ratios. With three specimens as a group, the arithmetic mean of the measured values of the three specimens was taken as the final test result.
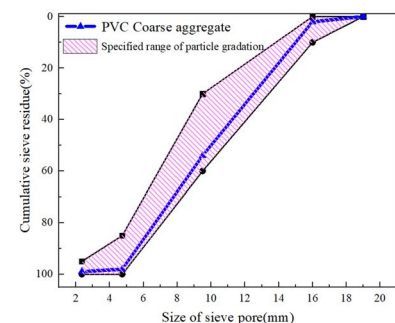
The specimens were made as follows: First of all, sand, stone and PVC coarse aggregate were poured into the mixer for dry mixing for 2 min. Second, add cement for dry mix for 2 min. Third, water was added for wet mixing for 2 min. Fourth, the mixed concrete was poured into a mold, and vibrated and molded on a vibrating table. Fifth, after standing for 24 h, the specimens were numbered and cured in the standard concrete (temperature 20 ± 2 ℃, humidity more than 95%) curing room for 28 days.

a PVC soft board before crushing   **b** Flaky PVC particles after crushing   **c** Grading curve of PVC aggregate

Fig. 1 PVC aggregate used in the test.

Hu *et al. Int J Concr Struct Mater*   (2021) 15:26

Page 4 of 16

Table 1 Concrete mixing ratio.

Specimen code	Cement (kg/m³)	Fine aggregate (kg/m³)	Coarse aggregate (kg/m³)	Water (kg/m³)	PVC Coarse aggregate(kg/m³)
NC	438	596	1156	210	0
CA5%	438	596	1098.1	210	14.1
CA10%	438	596	1040.2	210	28.2
CA15%	438	596	982.3	210	42.3
CA20%	438	596	924.4	210	56.4
CA30%	438	596	808.6	210	84.6

2.3 Test Instruments and Methods

1. Slump, cube compression and Brazilian splitting tests

   The experimental process of slump is shown in Fig. 2a. Suns WAW-2000 universal testing machine was employed to carry out uniaxial compression test of the cubic specimens at a loading rate of 0.042 mm/s, as shown in Fig. 2b. Using the splitting fixture as shown in Fig. 2c, the cylinder specimen was split at a loading rate of 0.005 mm/s.

2. Steel ball free falling impact test

   As the concrete specimen has energy absorption ability, the steel ball will rebound after hitting the specimen. The transient rebound phenomenon was captured using a NAC high-speed camera HX-3 made in Japan to study the energy absorption characteristics of the specimens under low-speed impact. According to the specifications of CECS02-2005, the simple impact test device was made, as shown in Fig. 3a. The gravity acceleration is 9.81 m/s2, the mass of the steel ball is 0.5 kg, diameter is 37 mm, the height of the initial falling point h_0 is 1.0 m, and the distance from the scale line (the center point of the specimen) is

7.5 cm. The rebound height h_1 is captured by a high-speed camera. In addition, considering the actual difficulty and small value of E_{t1} test, it is considered that the value is 0, and the influence of other external forces and different landing position of steel ball are ignored in the test process. The relevant calculation formula is as follows. The energy propagation process is shown in Fig. 3b.

$$\left.\begin{array}{l} E_{a1} = E_{p0} - E_{p1} - E_{t1} \\ E_{p0} = mgh_0 \\ E_{p1} = mgh_1 \\ E_{t1} = 0 \end{array}\right\}, \tag{1}$$

where, E_{a1} is the energy absorption value of the first impact; E_{p0} is the gravitational potential energy at the initial position, E_{p1} is the gravitational potential energy at the highest point of rebound, and E_{t1} is the transmitted energy through the concrete.

3. Split Hopkinson pressure bar (SHPB) impact test

   A Φ 74 mm SHPB test system was employed in the test (Fig. 4). The compression bar was made of high strength alloy steel with elastic modulus of 210GPa. The basic principle of the SHPB test was based on the
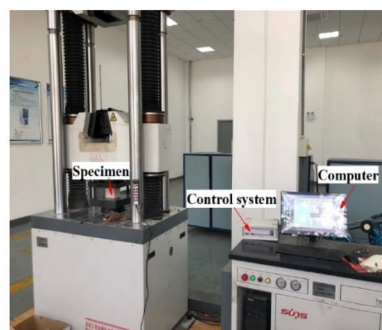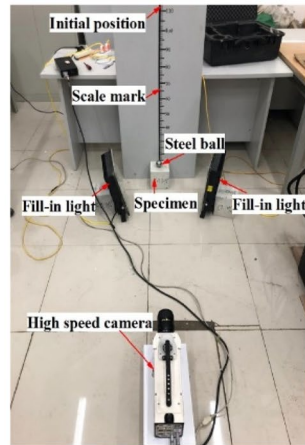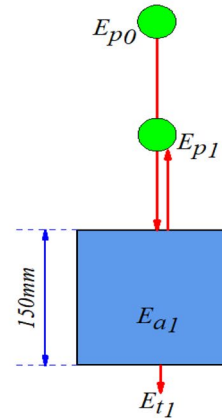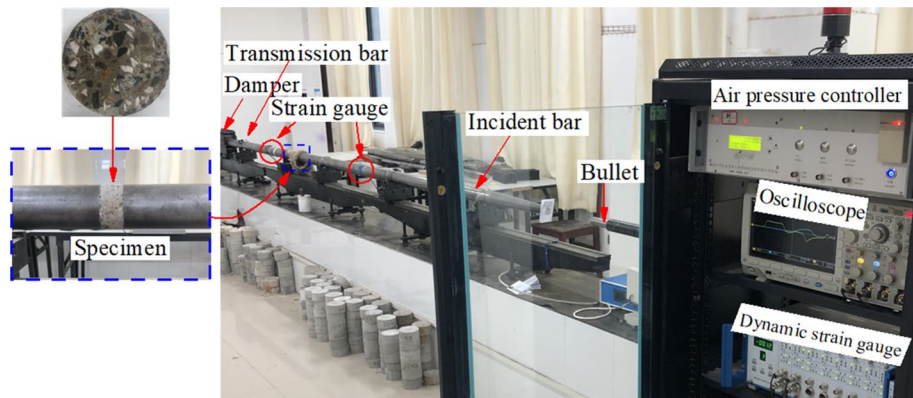

a Slump test   **b** Universal testing machine   **c** Splitting fixture

Fig. 2 Test instrument.

a Steel ball free falling impact test system   **b** Energy propagation process

Fig. 3 Impact test instrument and energy propagation sketch.

Fig. 4 SHPB system.

one-dimensional elastic stress wave assumption and the stress/strain uniformity assumption. The pulse signals were first collected by the strain gauges on the incident rod and the transmission rod, and then transformed to strain signals by the dynamic strain testing system. The stress, strain and strain rate of the impact compression were calculated according to Eq. (2) of three-wave method (Grote et al., 2001).

$$
\left.
\begin{aligned}
\sigma(t) &= \frac{A}{2A_s} E(\varepsilon_i + \varepsilon_r + \varepsilon_t) \\
\varepsilon(t) &= \frac{C}{L_s} \int_0^t (\varepsilon_i - \varepsilon_r - \varepsilon_t) dt \\
\overset{\bullet}{\varepsilon}(t) &= \frac{C}{L_s} (\varepsilon_i - \varepsilon_r - \varepsilon_t)
\end{aligned}
\right\},
\qquad (2)
$$

where $\sigma, \varepsilon, \overset{\bullet}{\varepsilon}$ are stress, strain and strain rate of the specimen, E, A, C are elastic modulus, cross-sectional area and wave velocity of the compression bar, A_s, L_s are the initial cross-sectional area and the initial length of the specimen, and $\varepsilon_i, \varepsilon_r, \varepsilon_t$ are incident strain, reflection strain and transmission strain in the compression bar.

The energy propagation process during the test is shown in Fig. 5, and the relevant energy calculation formula is as follows:

Hu *et al. Int J Concr Struct Mater*   (2021) 15:26

Page 6 of 16

Fig. 5 SHPB test energy propagation sketch.
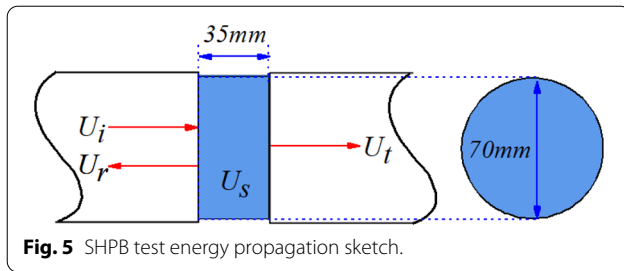
$$\left.\begin{aligned}
U_s &= U_i - U_r - U_t \\
U_i &= \frac{AC}{E}\int \sigma_i{}^2 \mathrm{dt} = \mathrm{AEC}\int \varepsilon_i{}^2 \mathrm{dt} \\
U_r &= \frac{AC}{E}\int \sigma_r{}^2 \mathrm{dt} = \mathrm{AEC}\int \varepsilon_r{}^2 \mathrm{dt} \\
U_t &= \frac{AC}{E}\int \sigma_t{}^2 \mathrm{dt} = \mathrm{AEC}\int \varepsilon_t{}^2 \mathrm{dt}
\end{aligned}\right\}, \quad (3)$$

where U_i, U_r, U_t represent the energy of incident wave, reflected wave and transmitted wave. U_s is the energy absorbed by the test piece; $\sigma_i, \sigma_r, \sigma_t$ are incident stress, reflection stress and transmission stress in the compression bar.

Test punching was carried out before the test. The test results are shown in Fig. 6. The concrete was not obviously damaged under the impact pressure of 0.2 MPa. However, the concrete was impacted and crushed into debris under the impact pressure of 0.75 MPa. Therefore, this study carried out different strain rate tests under the air pressures of 0.3 MPa, 0.4 MPa and 0.65 MPa. Vaseline was coated on both ends of the specimens to make them closely contact with the compression bar during the impact process. A simple waveform shaper was employed to reduce the dispersion effect during wave propagation and ensure uniform stress distribution in the specimens.
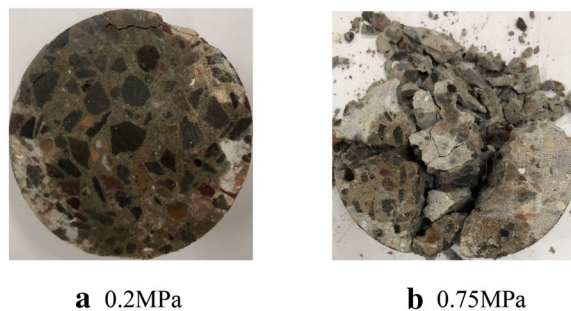
3 Results and Discussion

3.1 Slump, Mechanical Properties

Table 2 shows the slump and mechanical properties of concrete.

It can be found from Table 2 that the compressive strength and splitting strength decrease sharply with the increase of PVC aggregate content. When the content is 30%, the compressive strength is only 28.82 MPa and the splitting strength is 2.21 MPa.

Combined with the above phenomenon and the microstructure diagram in Fig. 7, it is found that the continuous decrease of the compressive strength is caused by the poor bonding effect and porosity of the interface transition zone between cement and PVC aggregate because of the side wall effect after adding PVC coarse aggregate into concrete (Ollivier et al., 1995), This is because there is less cement slurry near the PVC aggregate, which affects the hydration products. In addition, the water film of plastic surface treatment also blocks the bonding between cement and plastic particles. So, greater mixing amount of plastic particles can increase the weak interface, thus decreasing static and dynamic strength (Choi et al., 2005; Naik et al., 1996; Pham et al., 2020).

The elastic modulus also keeps decreasing, which indicates that the brittle failure of the specimen becomes ductile failure, and the integrity of the specimen becomes better, this is because PVC particles have good elastic deformation characteristics, which can store and consume part of the energy input from the outside in the form of elastic strain energy, which weakens the energy consumption through the fracture of cement mortar matrix structure, and has good integrity. The more the amount of PVC particles, the less the cracks and the smaller the gap. Therefore, with the increase of PVC aggregate content, the specimen is relatively more complete. The typical compression failure mode is shown in Fig. 8.

This is because the PVC aggregate used in this paper is flaky, irregular in shape, and the specific surface area increases, so the slump decreases. However, due to the

Fig. 6 Failure modes of NC specimens under different impact pressures.

Table 2 Slump and mechanical properties.

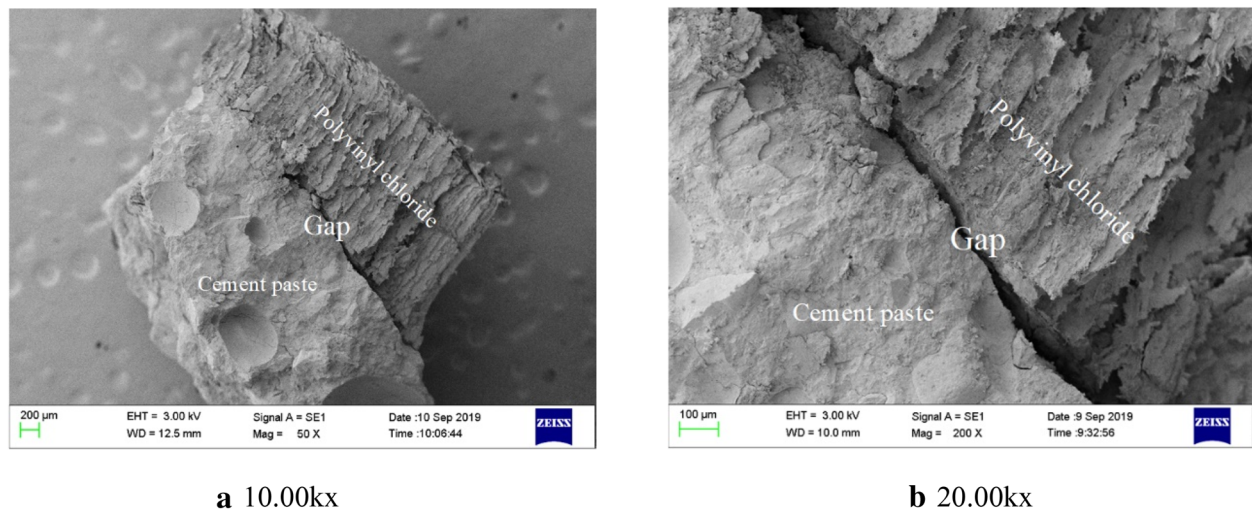| Specimen code	Compressive strength (MPa)	Elastic modulus (GPa)	Splitting strength (MPa)	Slump (mm)
NC	49.34	4.06	4.16	185
CA5%	43.32	3.97	3.37	181
CA10%	39.92	3.81	2.99	179
CA15%	38.3	3.44	2.76	171
CA20%	33.8	3.26	2.39	165
CA30%	28.82	2.91	2.21	160

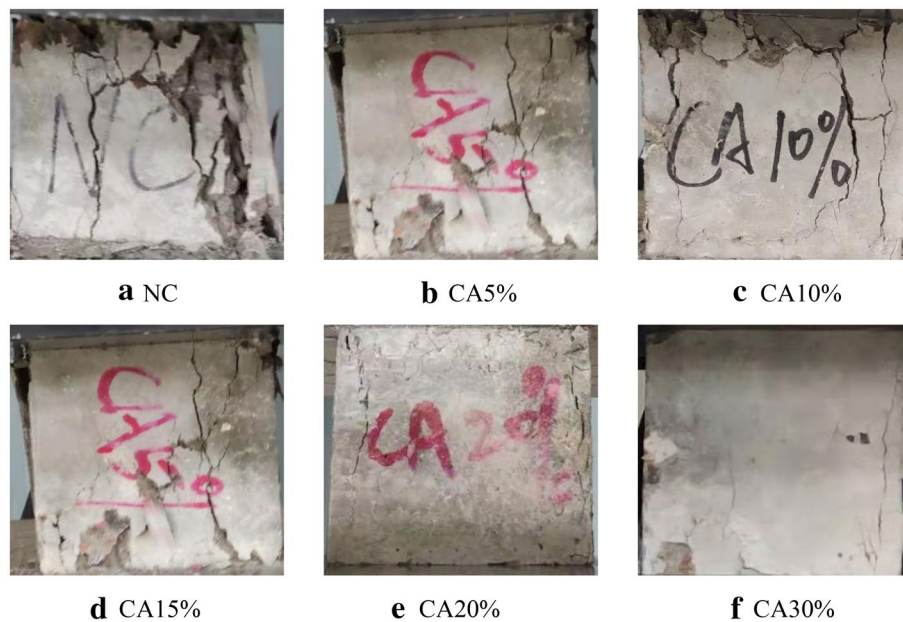**Fig. 7** Microstructure of CA30% at different magnification.

Fig. 8 Typical compression failure modes.

small amount, the decline trend is not obvious. The slump of concrete used in road engineering is required to be 140–160 mm, the slump of shotcrete is required to be 160–180 mm, and the slump of underwater cast-in-place pile is required to be 180–200 mm.

3.2 Steel Ball Free Falling Impact Test

The rebound height and the initial height were captured by the high-speed camera, and the rebound energy value and the energy absorption value of the specimen were calculated. To determine the relationship between the energy absorption characteristics of concrete under the free falling impact load of steel balls and the SHPB high-speed impact, the energy absorption rate (EAR) was defined to compare the energy absorption capacity of different specimens (Hu & Xu, 2020a, b). The equation is as follows:

$$\text{EAR}_1 = \frac{E_{a1}}{E_{p0}}, \tag{4}$$

Hu *et al. Int J Concr Struct Mater* (2021) 15:26

Page 8 of 16

where EAR_1 denotes the energy absorption rate of the first impact; E_{a1} denotes the energy absorption value of the first impact; E_{p0} denotes the gravitational potential energy at the initial position.

The transient phenomenon at the highest rebound point of steel balls was captured by the high-speed camera, as shown in Fig. 9. Due to the position of the scale, the actual rebound height is the scale value in the figure reduced by 14 cm. Therefore, when the mixing amount of the PVC aggregate is 0%, 5%, 10%, 15%, 20% and 30%, the corresponding rebound peak height is 16.5, 15.96, 14.3, 13.09, 10.5 and 8.91 cm. The above formula was used to calculate the rebound energy value, energy absorption values and energy absorption rate of the specimens. The detailed data are listed in Fig. 10.

As shown in Fig. 10, for different mixing amounts (0–30%), the energy absorption values of the steel balls under free falling impact are 4.1, 4.13, 4.21, 4.27, 4.39, and 4.47 J. The rebound height decreases with the increase of the mixing amount, but the energy absorption values increase, and the energy absorption rates are 83.59%, 84.2%, 85.83%, 87.05%, 89.5% and 91.13%, respectively. The energy absorption capacity has been significantly improved, because the flaky PVC particles have good deformation and bending properties. Also, after adding flaky PVC particles as elastic aggregates into concrete, the plastic–cement composite materials have good flexibility (Hu & Xu, 2020a, b; Li et al., 2019). There is a good

Fig. 10 Rebound energy value, energy absorption values and energy absorption rate.
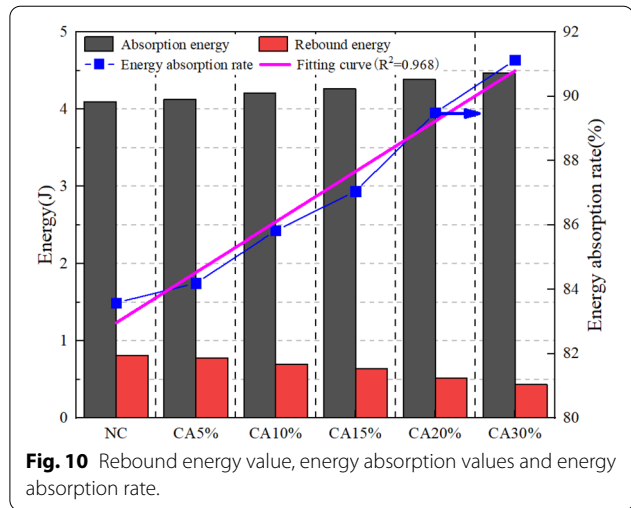
linear relationship between the energy absorption rate and the amount of PVC aggregate, and the relationship formula is $y = 0.271x + 83.265$, which is helpful for predicting the energy absorption characteristics of concrete with a large amount of PVC aggregate in the future.

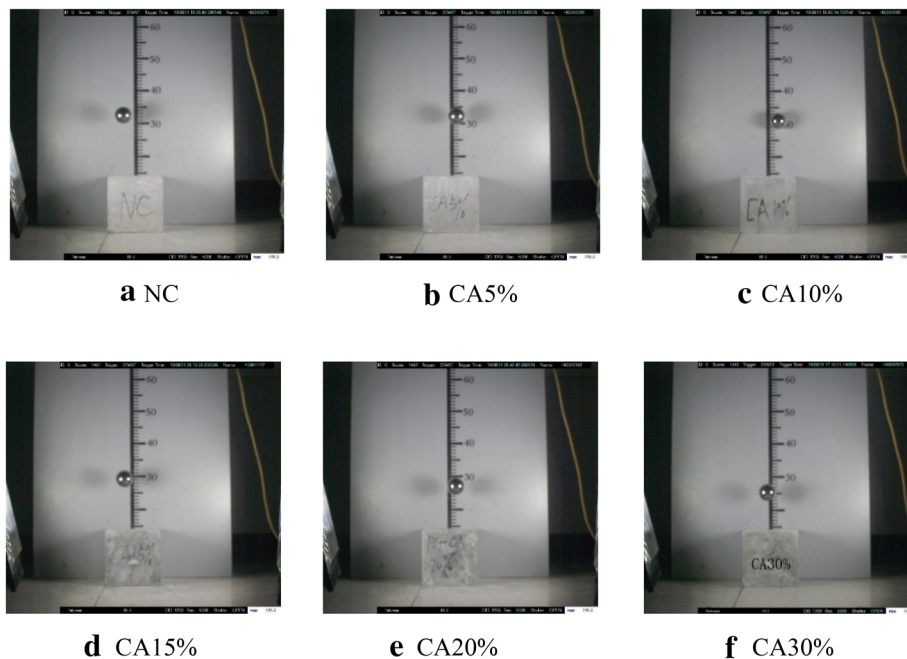### 3.3 SHPB Impact Test

(1) Static and dynamic compressive strength

a NC   **b** CA5%   **c** CA10%

d CA15%   **e** CA20%   **f** CA30%

Fig. 9 Transient phenomenon of the highest rebound point.

Hu *et al. Int J Concr Struct Mater*   (2021) 15:26

Page 9 of 16

Through calculation, the static and dynamic compressive strength of the specimens and the corresponding strain rates are presented in Fig. 11. In SHPB test, the strain rate of each specimen is the strain rate corresponding to the peak stress point (Grote et al., 2001; Huang et al., 2020; Pham et al., 2020). Because the loading rate is 2.5 mm/min in the static compressive strength test, in this study, the strain rate of the specimen is $4.2 \times 10{-}4 \ s^{-1}$.

Figure 11 shows the static compressive strength of the specimens with different mixing amounts (0–30%) is 49.34, 43.22, 39.92, 38.3, 33.8 and 28.82 MPa, respectively. Three impact air pressures were applied to carry out SHPB impact compression tests. For example, the three strain rates of NC are 46.6, 59.3, $95.4S^{-1}$, and the corresponding dynamic compressive strength is 56.59, 62.46 and 78.5 MPa, respectively.

With the increase of PVC aggregate content, the static compressive strength and the dynamic compressive strength of the concrete under the three kinds of impact pressures decrease significantly. The decreasing rate of the static compressive strength does not exceed 41.59%, while the decreasing rates of the dynamic compressive strength under the three impact pressures are not higher than 33.95, 34.93 and 30.99%, respectively. Despite the same impact pressure, the dynamic compressive strength of the specimens shows a complex change law due to different strain rates.

Regardless of the mixing amount of PVC aggregate (0–30%), the dynamic compressive strength of concrete is obviously enhanced with the increase of the strain rate. The concrete is damaged due to the generation and development of cracks. According to the principle of fracture mechanics, the energy required for crack generation is much greater than that required for crack development (Hillerborg et al., 1976). The greater the loading rate, the more cracks are generated in concrete, and the more energy needs to be dissipated. Under high strain rate, the impact load is applied for a short time, and the concrete cannot accumulate energy via plastic particle deformation. Consequently, the dissipation energy can only be provided by increasing the stress, and the compressive strength of concrete increases with the increase of the strain rate (Albano et al., 2009; Li et al., 2019). When the mixing amount is 30%, the dynamic compressive strength decreases by about 35%, and the static compressive strength is only 28.82 MPa.

The engineering background of this paper is shotcrete used in tunnel and coal mine roadway support. Generally, the compressive strength of shotcrete is not less than 25 MPa, but considers the size effect, accelerating agent (Min et al., 2014) and the strength decline caused by different curing conditions, and combining with the actual engineering, it is considered that only when the compressive strength of concrete under standard curing is not less than 30 MPa, such mixing ratio have the significance of engineering application. If only the strength performance is considered, the content of PVC coarse aggregate should not exceed 20%

(2) Failure mode of specimens

The SHPB impact compression failure modes of the concrete specimens vary obviously under different mixing amounts of PVC aggregate (0–30%). Figure 12 shows the typical failure modes of all specimens under the impact pressure of 0.4 MPa (52.1–67.1 S^{-1}) and NC specimens under the impact pressure of 0.3 MPa (46.6 S^{-1}), 0.65 MPa (95.4 S^{-1}).

Figure 12 show the NC specimens were seriously damaged under the impact pressure of 0.4 MPa (52.1–67.1S^{-1}), while the concrete specimens mixed with PVC aggregate have many microcracks on their surfaces after impact damage, but they are not scattered and remain complete (Fig. 12e). The relative integrity of the specimens after impact is positively correlated with the mixing amount of PVC aggregate. The higher the mixing amount, the more complete the specimens. The above phenomenon is resulted from the random distribution of PVC plastic particles in concrete, which bridge the
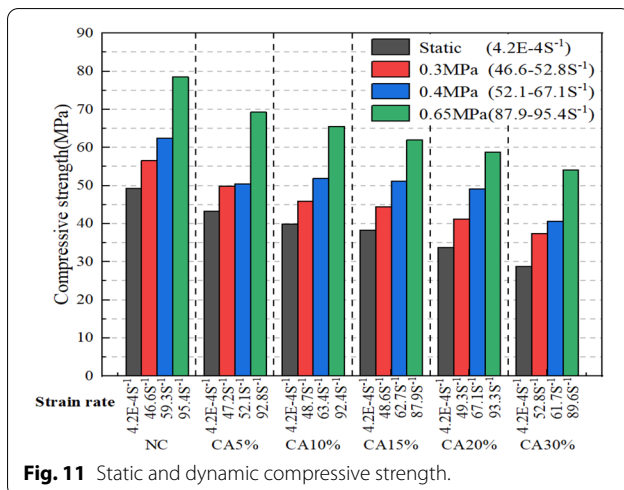

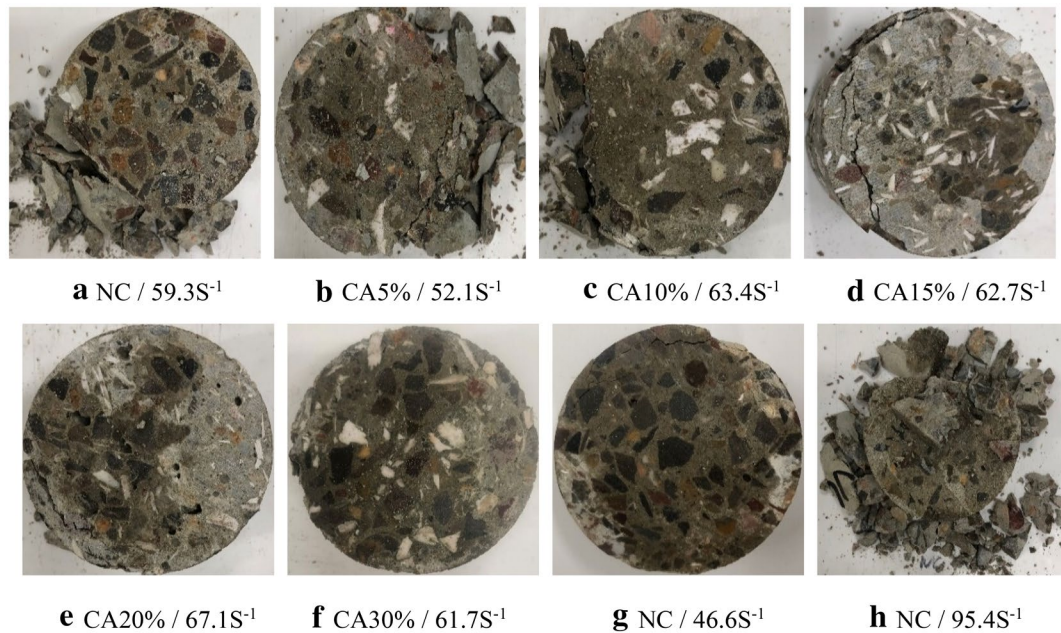**Fig. 11** Static and dynamic compressive strength.

Fig. 12 Typical failure modes of specimens.

Under the figure, labels:
a NC / 59.3S⁻¹ **b** CA5% / 52.1S⁻¹ **c** CA10% / 63.4S⁻¹ **d** CA15% / 62.7S⁻¹
e CA20% / 67.1S⁻¹ **f** CA30% / 61.7S⁻¹ **g** NC / 46.6S⁻¹ **h** NC / 95.4S⁻¹
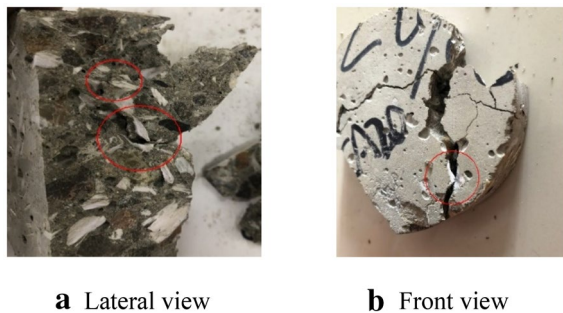

a Lateral view   **b** Front view
Fig. 13 PVC particle morphology on fracture surface.

concrete matrix (Fig. 13) and prevent crack propagation. Meanwhile, due to the smaller elastic modulus of the PVC plastic, it can not only bear, buffer and absorb some stress when the concrete is subjected to impact load, but also eliminate stress concentration, and restrict the generation and development of microcracks (Hu & Xu, 2020a, 2020b). In short, the integrity of the failure mode of the specimens can be equivalent to the impact resistance. Scholars have found that plastic concrete has good impact resistance, which also verifies the test conclusion of our study (Huang et al., 2020; Pham et al., 2020). With the increase of the strain rate, the failure mode of the NC specimen becomes more serious (Huang et al., 2020; Pham et al., 2020). Under

high strain rate, the main crack does not propagate, and the impact energy is absorbed by the microcracks and weak interfaces in the specimens, resulting in multi-point microcracks and serious damage. The specimens with other mixing amounts (5–30%) show similar failure law, which is not repeated here.
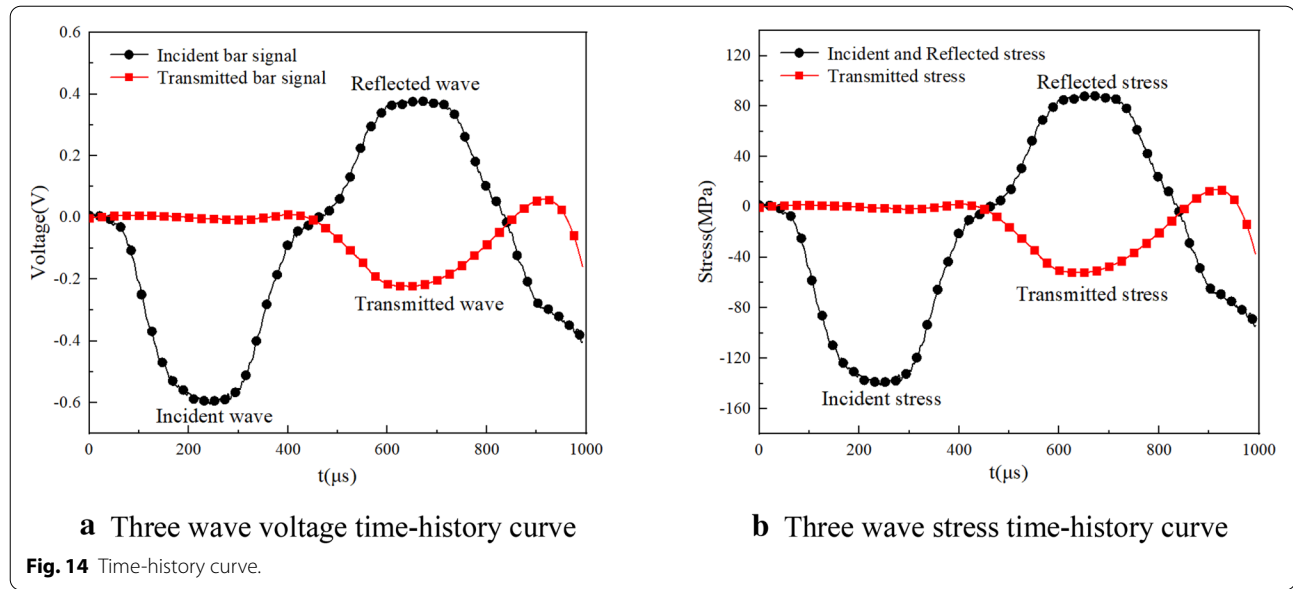
(3) Energy calculation

The voltage time-history curve derived from the testing machine is shown in Fig. 14a. Through Eqs. (5–6), the three-wave stress diagram is calculated as shown in Fig. 14b. According to the similar stress difference Eq. (7), the stress uniformity is calculated to ensure the accuracy of the experimental data. The final calculation result $\mu = \frac{2|84.91-89.11|}{|84.91+89.11|} \times 100\% = 4.82\% < 5\%$, meets the stress uniformity assumption, and the experimental data are accurate.

$$\varepsilon(t) = \frac{2\Delta U(t)}{K_1 K_2 U_0}, \tag{5}$$

$$\sigma(t) = E\varepsilon(t), \tag{6}$$

$$\mu = \frac{2|\sigma_1 - \sigma_2|}{|\sigma_1 + \sigma_2|} \times 100\%, \tag{7}$$

where K_1 is the sensitivity coefficient of the resistance strain gauge, with a value of 2.08%, K_2 is the magnification factor of the dynamic strain gauge, with a

a Three wave voltage time-history curve

b Three wave stress time-history curve

Fig. 14 Time-history curve.

value of 500, U_0 is the bridge pressure, with a value of 4. $\sigma_1 = \sigma_t - \sigma_i, \sigma_2 = \sigma_r$, where $\sigma_i, \sigma_r,$ and σ_t are the incident stress, the reflected stress and the transmitted stress, respectively.

To accurately measure the energy characteristics of the specimens, this study introduced specific energy absorption (SEA) (Li et al., 2000). The physical meaning of SEA is the energy absorbed by the unit volume of concrete specimen during impact compression. The equation is as follows:

$$SEA = \frac{U_s}{A_s L_s}. \tag{8}$$

The specific energy absorption value (NC specimen at 0.4 MPa impact pressure) was calculated in three steps: (1) the voltage time-history curve data derived from the testing machine were converted to the time-history curve of $\varepsilon_i{}^2, \varepsilon_r{}^2, \varepsilon_t{}^2$ in Fig. 15a according to Eqs. (5–6). (2) the time-history curve of U_i, U_r, U_t and U_s was obtained through integral computation based on the time-history curve obtained in the first step, as shown

a Square of strain time-history curve

b energy time-history curve
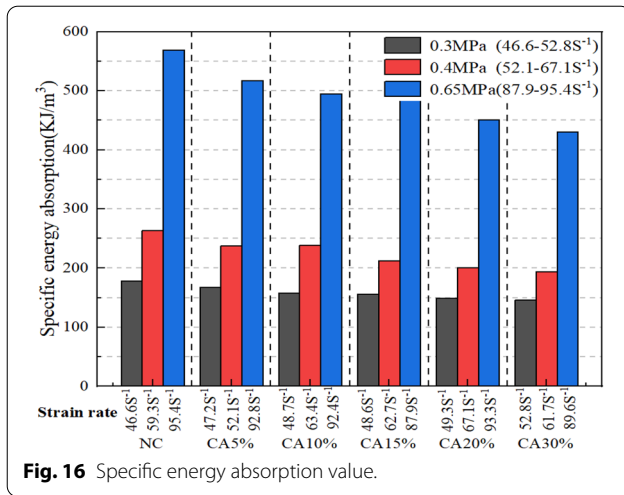
Fig. 15 Time-history curve.
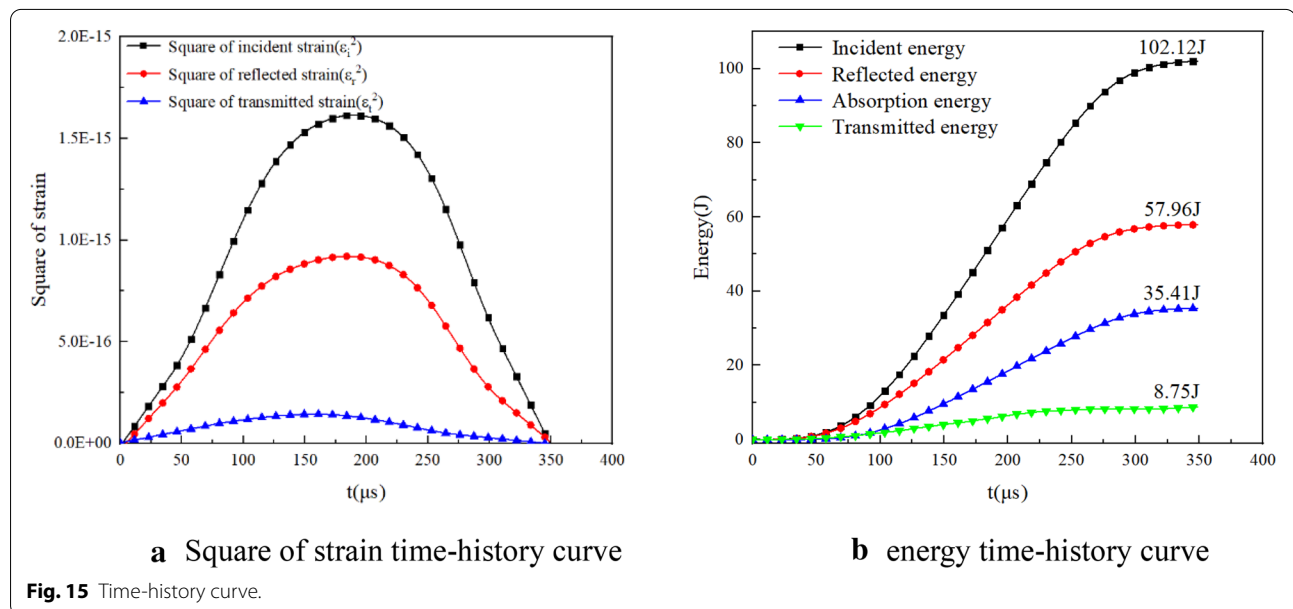
Fig. 16 Specific energy absorption value.

in Fig. 15b. (3) SEA was calculated according to Eq. (8). Square of strain time-history curve and energy time-history curve of the NC specimen at 0.4 MPa impact pressure are shown in Fig. 10, and the calculation process for other specimens is the same.

Through the above calculation, the SEA data of the specimens are shown in Fig. 16.

As can be seen from Fig. 16, the specific energy absorption values under the three different impact pressures decrease with the increase of PVC aggregate content. For example, under the impact pressure of 0.65 MPa (87.9–95.4 S^{-1}), the specific energy absorption value of CA30% specimen decreases by 24.43% compared with that of NC specimen. This is because adding PVC plastic particles can cause side wall effect of interface bonding (Fig. 7). Although elastic plastic particles can improve energy absorption, it cannot compensate for the negative impact of the strength reduction on energy absorption. However, since different specimens have different strain rates under the same impact pressure, the change law is complicated (Wang et al., 2010). Regardless of the mixing amount of PVC aggregate, the specific energy absorption value of the concrete increases obviously with the increase of the strain rate. For example, when the impact pressure is 0.65 MPa (93.3 S^{-1}), the specific energy absorption value of CA20% is 203% higher than that under 0.3 MPa (49.3 S^{-1}). In the case of high strain rate, the main crack does no propagate, and the impact energy is absorbed by the microcracks and weak interfaces in the specimens. More energy is absorbed to form multi-point microcracks, thereby leading to cracks. Huang et al., (2020) found that the static compressive strength is positively related to the energy absorption value, which is consistent with the conclusion of this study, and the test results are proved to be correct.

However, Pham et al. (2020) found that the energy absorption value calculated in the dynamic impact compression test can only characterize the real energy absorption of the specimen at a certain strain rate, but cannot reflect the real energy absorption capacity. Therefore, he divided the energy absorption value of the specimen by its static compressive strength, finding that the energy absorption value per MPa can truly reflect the energy absorption capacity of the specimen. Moreover, the closed area below the stress–strain curve was taken as the energy absorption value, and the corresponding unit KN/m^2 was the same as KJ/m^3 of the specific energy absorption value in this study (1 $J=1$ $N \times 1$ m), both of which became dimensionless numbers after being divided by the unit MPa.

Based on Pham et al. (2020) study results, this study took the ratio of specific energy absorption value to static cube compressive strength as the measurement index to investigate the energy absorption capacity of concrete specimens. The Eq. (9) is as follows, namely, the specific energy absorption values per MPa are shown in Fig. 17.

$$SEA_{per\text{-}MPa} = \frac{SEA}{f_{cu,k}}, \tag{9}$$

where $f_{cu,k}$ is 28d cube compressive strength of the concrete.

In Fig. 17, the specific energy absorption per MPa under the three different impact air pressures increases with the increase of the PVC aggregate content, indicating that the energy absorption capacity has been enhanced. For example, under the impact air pressure of 0.65 MPa (87.9–95.4S^{-1}), the energy absorption capacity of CA30% specimen is increased by 29.31% compared with that of NC specimen, which is resulted from the good elasticity, large deformation and energy
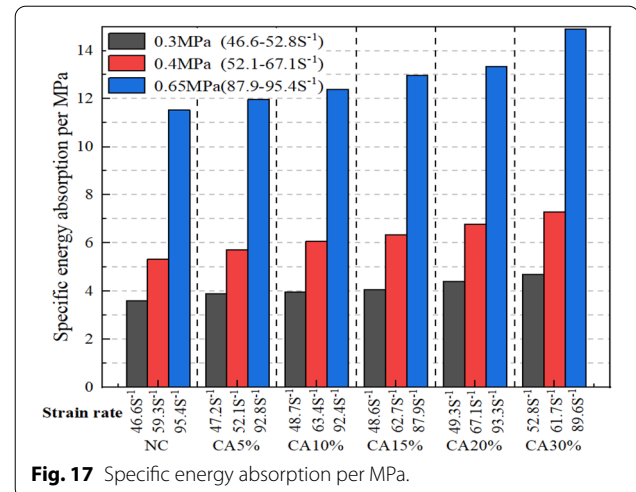

Fig. 17 Specific energy absorption per MPa.

absorption of the PVC coarse aggregate. Increasing the mixing amount of the PVC coarse aggregate can enhance the energy absorption potential of concrete. Under the same compressive strength, PVC coarse aggregate concrete can absorb more energy compared with ordinary concrete. Many scholars have tried adding silica powder, fiber or physically modified plastics to improve the compressive strength and enhance the actual energy absorption value (Elchalakani, 2015; Nili & Afroughsabet, 2010a, b; Shao et al. 2019; Xie et al. 2019). Regardless of the mixing amount of PVC aggregate, the specific energy absorption value per MPa increases obviously with the increase of the strain rate. The energy absorption capacity is in direct proportion to the strain rate. For example, the energy absorption capacity of CA30% under the impact pressure of 0.65 MPa is increased by 216% compared with that under 0.3 MPa (49.3 S^{-1}). The main crack does not develop under high strain rate, and the impact energy is absorbed by the microcracks and weak interfaces in the specimen. More energy will be absorbed, thus forming multi-point microcracks. The greater the strain rate, the more microcracks will be formed, and the stronger the energy absorption capacity (Pham et al., 2020).

The engineering background of this paper is shotcrete used in tunnel and coal mine roadway support. Generally, the compressive strength of shotcrete is not less than 25 MPa, but considers the size effect, accelerating agent (Min et al., 2014). and the strength decline caused by different curing conditions, and combining with the actual engineering, it is considered that only when the compressive strength of concrete under standard curing is not less than 30 MPa, such mixing ratio have the significance of engineering application.

Based on the above test data, to avoid serious strength loss and give full play to the advantages of PVC plastic particles such as light weight, elasticity, crack resistance and deformation in concrete, and meet the requirements of shotcrete slump (160–180 mm), the mixing amount of PVC coarse aggregate should not exceed 20%. In view of the fact that the energy absorption capacity is in direct proportion to the strain rate, the PVC coarse aggregate concrete under higher strain rate can be experimented in the future, such as flat blasting and light-gas gun penetration (Cusatis, 2011; Hao & Hao, 2014). In addition, considering the low strength and high energy absorption capacity of PVC concrete, composite modified reinforced PVC concrete can be further studied to improve its compressive strength, release its energy absorption capacity and increase the energy absorption value (Khan et al., 2018; Nili & Afroughsabet, 2010a, b).

3.4 Relationship Between Energy Absorption Characteristics Under Different Impact Loads

The actual energy absorption value of PVC coarse aggregate concrete shows completely different change rules under different impact loads. Establishing new evaluation indexes of energy absorption capacity under different impact loads helps to determine the relationship between energy absorption characteristics of concrete under steel ball free falling low-speed impact load and SHPB high-speed impact load, and fitting line of slope and intercept of fitting curve under high-speed impact as shown in Fig. 18.

a Fitting line of energy absorption characteristics under low-speed and high-speed impact

b Slope and intercept of the fitting line at different impact pressure

Fig. 18 Relationship between energy absorption characteristics under different impact loads.
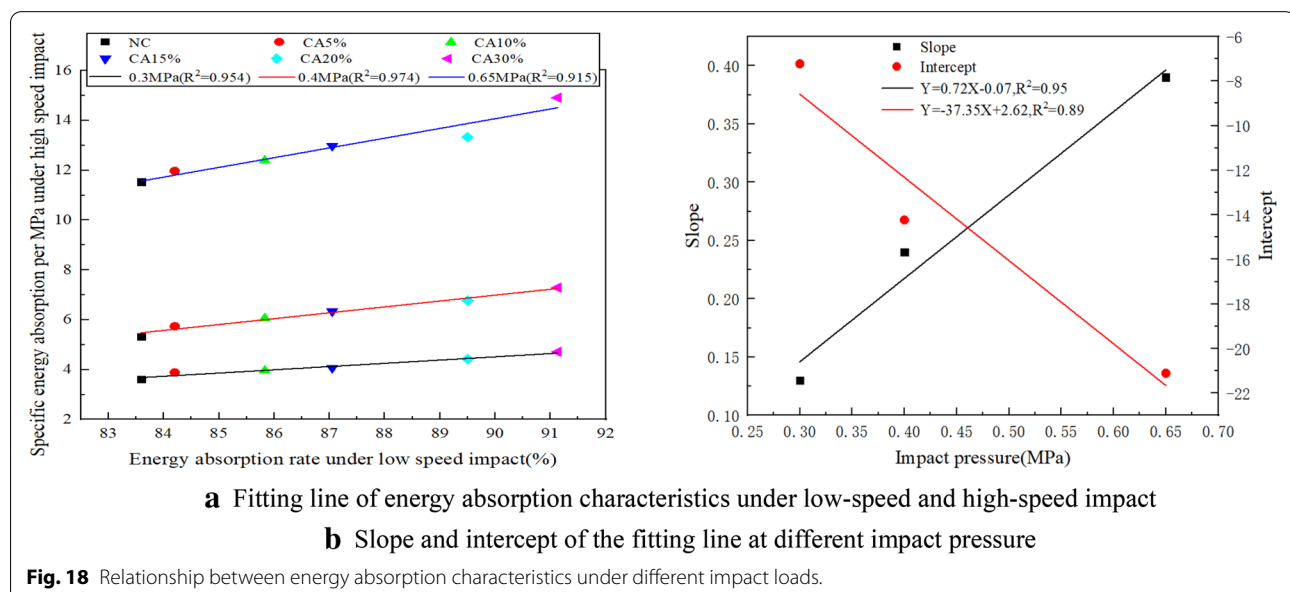
There is a good linear relationship between the energy absorption rate under steel ball free falling low-speed impact load and the specific energy absorption value per MPa under SHPB high-speed impact load. Particularly, the linear correlation coefficient is up to 0.974 at 0.4 MPa (52.1–$67.1\mathrm{S}^{-1}$). The greater the impact air pressure, the larger the slopes of the fitting straight lines, which are 0.13, 0.24 and 0.39, respectively. PVC coarse aggregate concrete may have better energy absorption effect at higher strain rate load (explosion, earthquake, etc.) (Hao & Hao, 2014).

Although the strain rates of different specimens vary at the same impact pressure, the energy absorption relationship under low-speed impact and high-speed impact can be used to predict the energy absorption characteristics under different PVC aggregate content or higher-speed impact pressure, which can provide important reference for safer, more economical, and environmental protection engineering structure design. The slope and intercept of the fitting line change linearly under different impact pressure. It can provide prediction basis and theoretical knowledge for future study of energy absorption characteristics of concrete under higher strain rate loads, and has great application significance in engineering.

4 Discussion

4.1 Influence of Different Curing Conditions on Performance

Different curing temperature and humidity have great influence on the performance of concrete specimens, because the temperature and humidity environment is the main factor that affects the hydration reaction degree and hydration reaction speed of cementitious materials. Too high curing temperature and too low curing humidity will cause damage to the concrete interior. And the standard concrete curing conditions are temperature 20 ± 2 ℃ and humidity more than 95%, which are completely different from the actual engineering curing conditions. In the research process, we should consider the changes of concrete performance caused by the standard curing and the actual engineering curing. According to the existing research, the actual engineering concrete strength is more than 20% lower than the standard curing, so we should consider this error when designing the strength of PVC aggregate concrete.

The hydration rate of concrete is faster in the early stage and slower in the later stage. It is also worth studying whether PVC aggregate will affect the early strength and whether the performance of concrete changes normally at different ages.

The existing research found that the change rule of concrete strength with age is $f_n = f_{28} \times \log_{10}^n / \log_{10}^{28}$, where n is the age value. The composition of ordinary concrete

and PVC aggregate concrete is different, and whether the rule is similar or not. Before determining the final mix proportion, we should consider the change rule of various properties of PVC aggregate concrete with time, so as to provide help for the safe application of the material.

4.2 Energy Calculation

In the steel ball free falling impact test, although the value of the transmitted energy through the concrete block is small, to avoid errors, the value should be removed when calculating the absorbed energy. Referring to the relevant literature (Wu et al., 2021), it is found that the method shown in Fig. 19 can be used to calculate the transmitted energy. The transmission force can be regarded as pulse load acting on the concrete cushion instantaneously. First, through the force sensor at the center of the concrete cushion and the displacement sensor at the middle of the span, the transmission force–displacement curve can be obtained, and then by calculating the curve area, the transmission energy can be roughly obtained. In addition, to avoid the ball impact point deviation, the sleeve can be used for positioning.

5 Conclusions

This study investigated the energy absorption characteristics and microstructure of PVC coarse aggregate concrete under impact load, and drew the following conclusions:

(1) With the increase of PVC aggregate content, the compressive strength and splitting strength of concrete decrease sharply, while the elastic modulus and slump decrease slowly.

(2) The dynamic compressive strength of the concrete under impact pressures of 0.3, 0.4 and 0.65 MPa decreases obviously with the increase of the mixing amount of PVC aggregate (0–30%). The decrease
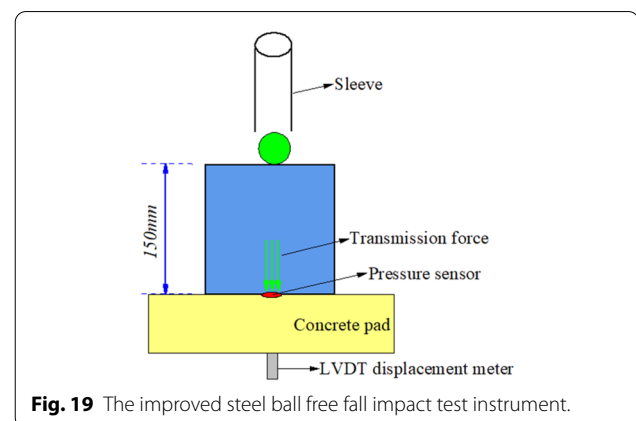

Fig. 19 The improved steel ball free fall impact test instrument.

Hu *et al. Int J Concr Struct Mater* (2021) 15:26

Page 15 of 16

rates of the dynamic compressive strength under the three different impact pressures are not higher than 33.95%, 34.93% and 30.99%, respectively. Regardless of the mixing amount of PVC aggregate, the dynamic compressive strength of the concrete increases substantially with the increase of the strain rate. Under the impact pressure of 0.65 Mpa, the dynamic compressive strength of 30% PVC aggregate content is 54.17 mpa, which is 87.96% higher than the static compressive strength.

(3) After the uniaxial compression test or the SHPB impact test, the relative integrity of the specimens is positively correlated with the mixing amount of the PVC aggregate. Moreover, the specimens are increasingly seriously damaged with the increase of the impact strain rate.

(4) Under the steel ball free falling low-speed impact load, the energy absorption rate of the concrete increases significantly as more PVC coarse aggregate is added. When the mixing amount is 30%, the energy absorption rate is 91.13%, which is 9.02% higher than that of the reference group, and the energy absorption capacity is improved significantly. Under the SHPB high-speed impact load, the specific energy absorption value per MPa increases with the increase of the mixing amount of PVC aggregate, 29.31–36.77% higher than that of the reference group. Moreover, regardless of the mixing amount of PVC aggregate, the specific energy absorption value per MPa increases significantly with the increase of the strain rate. The greater the strain rate, the stronger the energy absorption capacity.

(5) When the PVC aggregate content is 20%, the compressive strength and splitting strength of concrete are 33.8 MPa and 3.26 MPa, respectively, the slump is 165 mm, the energy absorption rate under low-speed impact is 89.5%, the dynamic compressive strength under 0.65 Mpa impact air pressure is 58.77 mpa, and the specific energy absorption value per MPa is 13.33, which meets the requirements of shotcrete used in tunnel, roadway support and other impact loads. Therefore, to give full play to the lightweight, elastic, crack resistance and effective energy absorption of PVC plastic particles in concrete, the content of PVC coarse aggregate should not exceed 20%.

(6) There is a good linear relationship between the energy absorption rate of the concrete under steel ball free falling low-speed impact and the specific energy absorption value per MPa under the SHPB high-speed impact. The greater the impact pressure, the larger the slopes of the fitting straight lines, which are 0.13, 0.24 and 0.39, respectively. The slope and intercept of the fitting line have a good linear relationship with the impact pressure.

Although PVC coarse aggregate concrete has stronger energy absorption capacity under impact load, the actual energy absorption value of the specimens is relatively low because of the poor compressive strength. Therefore, it is necessary to study composite modified reinforced PVC concrete in the future, expecting to give full play to the energy absorption capacity of PVC coarse aggregate concrete. Meanwhile, the energy absorption characteristics of PVC coarse aggregate concrete under higher strain rate load (explosion, earthquake, etc.) are worthy of further exploration.

Authors' contributions
SH wrote the manuscript and revised the manuscript, HT completed the method design, SH completed background investigation and data curation. All authors read and approved the final manuscript.

Author's information
Shi Hu is Ph.D in School of Civil Engineering and Architecture, Anhui University of Science and Technology, No. 168 Taifeng Road, Huainan 232001, China. Huaming Tang is graduate student in School of Civil Engineering and Architecture, Anhui University of Science and Technology, No. 168 Taifeng Road, Huainan 232001, China. Shenyao Han is graduate student in School of Civil Engineering and Architecture, Anhui University of Science and Technology, No. 168 Taifeng Road, Huainan 232001, China.

Declarations

References
Albano, C., Camacho, N., Hernandez, M., Matheus, A., & Gutierrez, A. (2009). Influence of content and particle size of waste pet bottles on concrete behavior at different w/c ratios. *Waste Management, 29*(10), 2707–2716
Al-Tayeb, M. M., Ismail, H., Dawoud, O., Wafi, S. R., & Al Daoor, I. (2017). Ultimate failure resistance of concrete with partial replacements of sand by waste plastic of vehicles under impact load. *International Journal of Sustainable Built Environment, 6*(2), 610–616
Bui, N. K., Satomi, T., & Takahashi, H. (2018). Recycling woven plastic sack waste and PET bottle waste as fiber in recycled aggregate concrete: An experimental study. *Waste management, 78*, 79–93

Cao, M., Li, L., Zhang, C., & Feng, J. (2018). Behaviour and damage assessment of a new hybrid-fibre-reinforced mortar under impact load. *Magazine of Concrete Research, 70*(17), 905–918

Chen, X.-Y., Ding, Y.-N., & Azevedo, C. (2011). Combined effect of steel fibres and steel rebars on impact resistance of high performance concrete. *Journal of Central South University of Technology, 18*(5), 1677

Choi, Y.-W., Moon, D.-J., Chung, J.-S., & Cho, S.-K. (2005). Effects of waste PET bottles aggregate on the properties of concrete. *Cement Concrete Research, 35*(4), 776–781

Cusatis, G. (2011). Strain-rate effects on concrete behavior. *International Journal of Impact Engineering, 38*(4), 162–170

Elchalakani, M. (2015). High strength rubberized concrete containing silica fume for the construction of sustainable road side barriers. *Structures, 1*, 20–38

Feng, W., Liu, F., Yang, F., Li, L., & Jing, L. (2018). Experimental study on dynamic split tensile properties of rubber concrete. *Construction and Building Materials, 165*, 675–687

Grote, D., Park, S., & Zhou, M. (2001). Dynamic behavior of concrete at high strain rates and pressures: I. experimental characterization. *International Journal of Impact Engineering, 25*(9), 869–886

Hao, Y., & Hao, H. (2014). Influence of the concrete DIF model on the numerical predictions of RC wall responses to blast loadings. *Engineering Structures, 73*, 24–38

Hillerborg, A., Modéer, M., & Petersson, P.-E. (1976). Analysis of crack formation and crack growth in concrete by means of fracture mechanics and finite elements. *Cement concrete research, 6*(6), 773–781

Hu, S., & Xu, Y. (2020a). Mechanical and energy absorption performances of concrete with good gradation recycled PVC aggregate. *Engineering Plastics Application, 48*(1), 90–94 (in Chinese).

Hu, S., & Xu, Y. (2020b). Preparation, performance test, and microstructure of composite modified reinforced concrete. *Advances in Civil Engineering, 2020*, 1–14

Huang, Z., Sui, L., Wang, F., Du, S., Zhou, Y., & Ye, J. (2020). Dynamic compressive behavior of a novel ultra-lightweight cement composite incorporated with rubber powder. *Composite Structures, 224*, 112300

Khan, M. Z. N., Hao, Y., Hao, H., & Shaikh, F. U. A. (2018). Experimental evaluation of quasi-static and dynamic compressive properties of ambient-cured high-strength plain and fiber reinforced geopolymer composites. *Construction and Building Materials, 166*, 482–499

Li, H.-L., Xu, Y., Chen, P.-Y., Ge, J.-J., & Wu, F. (2019). Impact energy consumption of high-volume rubber concrete with silica fume. *Advances in Civil Engineering, 2019*, 1–11

Li, Q., Zhao, X., Xu, S., & Gao, X. (2016). Influence of steel fiber on dynamic compressive behavior of hybrid fiber ultra high toughness cementitious composites at different strain rates. *Construction Building Materials, 125*, 490–500

Li, X., Lok, T., Zhao, J., & Zhao, P. (2000). Oscillation elimination in the Hopkinson bar apparatus and resultant complete dynamic stress–strain curves for rocks. *International Journal of Rock Mechanics and Mining Sciences, 37*(7), 1055–1060

Min, T.-B., Cho, I.-S., Park, W.-J., Choi, H.-K., & Lee, H.-S. (2014). Experimental study on the development of compressive strength of early concrete age using calcium-based hardening accelerator and high early strength cement. *Construction Building Materials, 64*, 208–214

Mohammed, A. A., Mohammed, I. I., & Mohammed, S. A. (2019). Some properties of concrete with plastic aggregate derived from shredded PVC sheets. *Construction and Building Materials, 201*, 232–245

Naik, T. R., Singh, S. S., Huber, C. O., & Brodersen, B. S. (1996). Use of post-consumer waste plastics in cement-based composites. *Cement Concrete Research, 26*(10), 1489–1492

Nili, M., & Afroughsabet, V. (2010a). Combined effect of silica fume and steel fibers on the impact resistance and mechanical properties of concrete. *International Journal of Impact Engineering, 37*(8), 879–886

Nili, M., & Afroughsabet, V. (2010b). The effects of silica fume and polypropylene fibers on the impact resistance and mechanical properties of concrete. *Construction Building Materials, 24*(6), 927–933

Ollivier, J., Maso, J., & Bourdette, B. (1995). Interfacial transition zone in concrete. *Advanced cement based materials, 2*(1), 30–38

Opon, J., & Henry, M. (2019). An indicator framework for quantifying the sustainability of concrete materials from the perspectives of global sustainable development. *Journal of Cleaner Production, 218*, 718–737

Pham, T. M., Chen, W., Khan, A. M., Hao, H., Elchalakani, M., & Tran, T. M. (2020). Dynamic compressive properties of lightweight rubberized concrete. *Construction and Building Materials, 238*, 117705

Saxena, R., Siddique, S., Gupta, T., Sharma, R. K., & Chaudhary, S. (2018). Impact resistance and energy absorption capacity of concrete containing plastic waste. *Construction Building Materials, 176*, 415–421

Senhadji, Y., Siad, H., Escadeillas, G., Benosman, A. S., Chihaoui, R., Mouli, M., & Lachemi, M. (2019). Physical, mechanical and thermal properties of lightweight composite mortars containing recycled polyvinyl chloride. *Construction Building Materials, 195*, 198–207

Shao, R., Wu, C., Su, Y., Liu, Z., Liu, J., & Xu, S. (2019). Numerical analysis on impact response of ultra-high strength concrete protected with composite materials against steel ogive-nosed projectile penetration. *Composite Structures, 220*, 861–874

Siddique, R., Khatib, J., & Kaur, I. (2008). Use of recycled plastic in concrete: a review. *Waste management, 28*(10), 1835–1852

Wang, L.-L., Zhou, F.-H., Sun, Z.-J., Wang, Y.-Z., & Shi, S.-Q. (2010). Studies on rate-dependent macro-damage evolution of materials at high strain rates. *International Journal of Damage Mechanics, 19*(7), 805–820

Wu, J., Hu, X., Mei, X., Xu, Z., Luo, G., & Han, M. (2021). Dynamic response of composite structure of concrete slab and buffer layer impacted by rockfall. *Hydrogeology and engineering geology, 48*(01), 78–87 (in Chinese).

Xie, J., Li, J., Lu, Z., Li, Z., Fang, C., Huang, L., & Li, L. (2019). Combination effects of rubber and silica fume on the fracture behaviour of steel-fibre recycled aggregate concrete. *Construction and Building Materials, 203*, 164–173

Xuan, W. H., Yang, G., & Chen, Y. Z. (2019). Study on dynamic mechanical performance of concrete containing recycled plastic particles. *Water Resources and Hydropower Engineering, 50*(11), 160–165 (in Chinese).

Publisher's Note